Kinematic Mapping Based Assembly Mode Evaluation of Planar Four-Bar Mechanisms

Hans-Peter Schröcker * Manfred L. Husty*
J. Michael McCarthy†

June 20, 2006

This paper presents a new method to determine if two task positions used to design a four-bar linkage lie on separate assembly modes (circuits) of a coupler curve, known as a "assembly mode defect." The proposed approach uses the image space of a kinematic mapping to provide a geometric environment for both the synthesis and analysis of four-bar linkages. The devised algorithm allows assembly mode decisions at an early design stage without resorting to the mechanism dimensions. The numerical effort is low compared to existing solutions.

1 Introduction

An important problem in the five-position synthesis of planar four-bar linkages is the separation of task positions due to a discontinuous coupler curve, which is termed "assembly mode defect." If less than five positions are specified for the design problem then there is a manifold of design solutions. Conditions that identify branching intersect this manifold to define regions of successful solutions. This is called *solution rectification*, see Waldron and Stevenson [20] and Gupta [7]. Prentis [11] provides a detailed presentation of the theory that underlies this approach.

Another approach to solution rectification is to use optimization theory to design the complete four-bar linkage system with branching conditions imposed as constraints on the solution, Schaefer and Kramer [13] and DaLio et al. [4].

Our goal is a formulation of solution rectification in a kinematic image space introduced by Blaschke [1] and Grünwald [6]. Bottema and Roth [2] utilize the kinematic image space for the study of the coupler movement of four-bar linkages. Ravani and Roth [12] formulate the four-bar linkage synthesis problem in this image space, which

*Institute of Basic Sciences in Engineering, Unit Geometry and CAD, University Innsbruck, A-6020 Innsbruck, Austria
†Department of Mechanical Engineering, University of California, Irvine, California 92697

has also been the focus of recent study by Hayes and Zsombor-Murray [8], Perez and McCarthy [10] and Brunnthaler et al. [3]. In this image space, the coupler movement of the resulting four-bar linkage generates an image curve with one or two branches, reflecting the properties of the coupler curve.

In what follows, we develop simple formulas that use this kinematic image space formulation to evaluate directly whether two task positions lie on a single branch of the image curve of a candidate design. In contrast to existing methods (Mirth and Chase [9], Waldron [18] or Waldron and Strong [19]) our approach eliminates the necessity to compute the mechanism's dimensions and crank angles (possibly after mechanism inversion) for the prescribed poses. This is desirable in connection with kinematic mapping based synthesis methods.

2 Four-bar motions in kinematic image space

In the projective extension P^3 of Euclidean three space we use homogeneous coordinates $[x_0, x_1, x_2, x_3]^T$ for describing points. Homogeneous coordinates are related to Euclidean coordinates $(x, y, z)^T$ via

$$x = \frac{x_1}{x_0}, \quad y = \frac{x_2}{x_0}, \quad z = \frac{x_3}{x_0}, \quad \text{if } x_0 \neq 0. \tag{1}$$

If $x_0 = 0$, the homogeneous coordinate vector describes a point at infinity. We identify the Euclidean plane with the plane $z = 0$ of a three dimensional space.

The kinematic mapping $\varkappa$ maps the planar displacements $\mathcal{D} \in \mathrm{SE}_2$ to points of P^3. If $\mathcal{D}$ is described by

$$\mathcal{D}\colon \begin{bmatrix} 1 \\ x' \\ y' \end{bmatrix} = \begin{bmatrix} 1 & 0 & 0 \\ a & \cos\varphi & -\sin\varphi \\ b & \sin\varphi & \cos\varphi \end{bmatrix} \cdot \begin{bmatrix} 1 \\ x \\ y \end{bmatrix}, \tag{2}$$

its kinematic image is the point

$$\varkappa(\mathcal{D}) = \left[2\cos\tfrac{\varphi}{2}, a\sin\tfrac{\varphi}{2} - b\cos\tfrac{\varphi}{2}, a\cos\tfrac{\varphi}{2} + b\sin\tfrac{\varphi}{2}, 2\sin\tfrac{\varphi}{2}\right]^T \in P^3. \tag{3}$$

It was shown in Bottema and Roth [2, Chapter 11] that the kinematic image of a four-bar motion is the intersection curve C of two hyperboloids $\mathcal{H}_1$, $\mathcal{H}_2 \subset P^3$. Suppose now that the four-bar has been synthesized from a certain number of precision points $\mathbf{p}_i \in C$. These points describe poses of the coupler during the four-bar motion. We want to decide if the given poses belong to different assembly modes of the synthesized four-bar mechanism.

The mechanism that corresponds to C has two assembly modes if and only if C has two branches (disconnected components). The input poses lie in different assembly modes, if their kinematic images $\mathbf{p}_i$ lie on both branches of C. For the synthesis of a finite number of four-bar mechanisms five precision points $\mathbf{p}_i$ are needed but in order to solve the assembly branch problem, it is sufficient to give an algorithm for deciding whether two given precision points lie on the same branch of C.

For the rest of this paper we restrict ourselves to the case of a non-degenerate intersection curve C. Other cases (rational or decomposed intersection curve) may occur but can be eliminated by well-known tests (Bottema and Roth [2, Chapter 11]).

3 The number of assembly modes

The assembly mode problem is a special case of the more general question: Decide whether two points $\mathbf{q}_1$, $\mathbf{q}_2$ on the intersection curve C of two quadrics in P^3 lie on the same or on different branches of C. To the best of our knowledge, this problem is not yet completely solved.

The first question to answer is, whether C consists of one component or two disconnected components. This problem has been solved in Tu et al. [16, Theorem 5] (see also Tu et al. [17]). Additionally, in this paper the notion of affinely finite or infinite intersection curves is introduced. We recall this definition because it is of major importance for the problem at hand.

Definition 1. A subset S of P^3 is called *affinely infinite* if every plane of P^3 intersects it in real points and *affinely finite* otherwise.

Theorem 1 (see Tu et al. [16])**.** *Let $\mathcal{A}$ and $\mathcal{B}$ be two real quadrics in P^3 with respective equations $\mathbf{x}^T \cdot \mathbf{A} \cdot \mathbf{x} = 0$ and $\mathbf{x}^T \cdot \mathbf{B} \cdot \mathbf{x} = 0$ where $\mathbf{x} = [x_0, x_1, x_2, x_3]^T$ and $\mathbf{A}$ and $\mathbf{B}$ are symmetric four by four matrices. We assume that the intersection of $\mathcal{A}$ and $\mathcal{B}$ is not degenerate and consider the polynomial $f(t) = \det(t\mathbf{A} + \mathbf{B})$ in t of degree four.*

1. *The intersection curve C of $\mathcal{A}$ and $\mathcal{B}$ has two affinely finite connected components or no real points in P^3 if and only if $f(t) = 0$ has four distinct real roots.*
2. *C has one affinely finite connected component in P^3 if and only if $f(t) = 0$ has two distinct real roots and a pair of conjugate complex roots.*
3. *C has two affinely infinite connected components in P^3 if and only if $f(t) = 0$ has two distinct pairs of complex conjugate roots.*

Theorem 1 enumerates all possible cases and all of them are of relevance to the investigations of the present paper (Figure 1). The only configuration that can be excluded is that of a purely imaginary intersection curve (because the precision points are real points of C). Note that roots of multiplicity two or more indicate degenerate intersection curves (Sommerville [15]) and will be excluded from the following investigations.

We can use Theorem 1 with $\mathcal{A} = \mathcal{H}_1 \colon \mathbf{x}^T \cdot \mathbf{H}_1 \cdot \mathbf{x} = 0$ and $\mathcal{B} = \mathcal{H}_2 \colon \mathbf{x}^T \cdot \mathbf{H}_2 \cdot \mathbf{x} = 0$ to decide whether C has one or two connected components. If only one connected component exists (two real roots) nothing else has to be done. If two affinely finite or infinite components exist, further investigation is needed. All these cases are also summarized in Table 1 which shows the connection between the number of real roots of $\det(t\mathbf{H}_1 + \mathbf{H}_2)$ and the number of assembly modes of the corresponding mechanism.

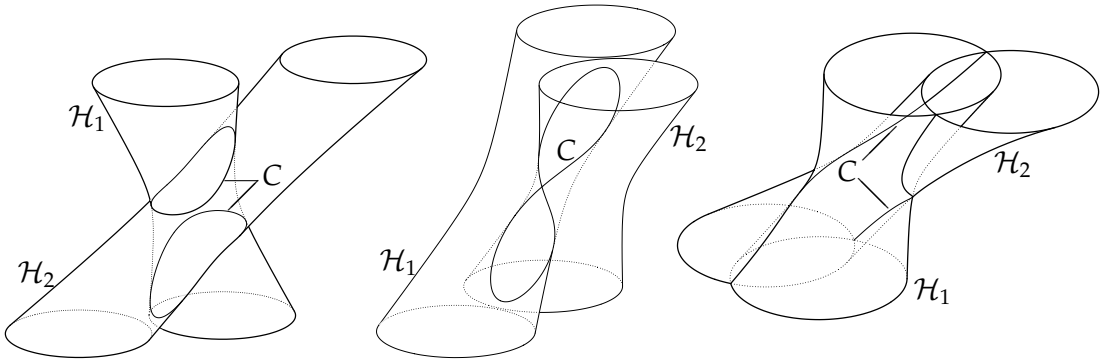

Figure 1: The intersection curve C has two affinely finite branches, one branch or two affinely infinite branches.

Remark 1. The relation between the number of real roots of $\det(t\mathbf{H}_1 + \mathbf{H}_2)$ and the number of assembly modes of the corresponding four-bar mechanisms is already mentioned in Bottema and Roth [2, Chapter 11.8]. However, the authors wrongly state that zero real roots would lead to only one assembly mode.

Theorem 1 is rather general, in fact too general for our purpose. The two hyperboloids $\mathcal{H}_i$ to be intersected have rather special geometric properties that can be exploited to simplify the criteria of Theorem 1. Instead of having to compute the roots of a polynomial of degree four, we will show that it is sufficient to solve two explicitly given polynomials of degree two. As an additional benefit, their roots can be used directly in the subsequent branch investigation.

We consider all Euclidean displacements that move a certain fixed point $(a, b)^T$ onto a circle with center $(\xi, \eta)^T$ and radius ϱ. With respect to a suitable coordinate frame in the fixed system, the equation of the kinematic image $\mathcal{H}$ of these transformations has the homogeneous equation

$$\mathcal{H}\colon \mathbf{x}^T \cdot \mathbf{H} \cdot \mathbf{x} = 0 \tag{4}$$

where

$$\mathbf{H} = \begin{bmatrix} (a-\xi)^2 + (b-\eta)^2 - \varrho^2 & 2\eta - 2b & 2a - 2\xi & 2b\xi - 2a\eta \\ 2\eta - 2b & 4 & 0 & -2a - 2\xi \\ 2a - 2\xi & 0 & 4 & -2b - 2\eta \\ 2\xi b - 2\eta a & -2a - \xi & -2b - \eta & (a+\xi)^2 + (b+\eta)^2 - \varrho^2 \end{bmatrix} \tag{5}$$

and

$$a,\ b,\ \xi,\ \eta,\ \varrho \in \mathbb{R}. \tag{6}$$

The kinematic image is a hyperboloid whose horizontal sections $z = \text{const.}$ are circles $S(z)$ with centers

$$\mathbf{m}(z) = 1/2 \begin{pmatrix} b - \eta + z(a + \xi) \\ -a + \xi + z(b + \eta) \\ 2z \end{pmatrix} \tag{7}$$

and squared radii

$$r^2(z) = 1/4\,\varrho^2(1+z^2). \tag{8}$$

In a four-bar motion the endpoints of the two arms run on circles, therefore the kinematic image of a four-bar motion is the intersection curve C of two hyperboloids $\mathcal{H}_1$, $\mathcal{H}_2$ of the special type (5).

Two circles $S_1(z)$, $S_2(z)$, each on one of the hyperboloids at a certain height, have either zero, one or two real intersection points. We turn our attention to those values of z where $S_1(z)$ and $S_2(z)$ have exactly one point in common because they correspond to planes that separate branches of C. In order to compute them, we have to solve the circle tangent conditions

$$\begin{aligned} T_1(z) &:= \|\mathbf{m}_1(z) - \mathbf{m}_2(z)\|^2 - (r_1(z) + r_2(z))^2 = 0, \\ T_2(z) &:= \|\mathbf{m}_1(z) - \mathbf{m}_2(z)\|^2 - (r_1(z) - r_2(z))^2 = 0, \end{aligned} \tag{9}$$

where we assume that $r_1^2(z) \geq r_2^2(z)$ for all $z \in \mathbb{R}$. This assumption is possible without loss of generality since the ratio of $r_1^2(z)$ and $r_2^2(z)$ is independent of z. The first circle tangent condition characterizes exterior, the second interior tangency.

The functions $r_1(z)$ and $r_2(z)$ are irrational. Nonetheless the equations in (9) are quadratic in z. Hence, there exist four (possibly complex) values z_1, z_2, z_3, z_4 such that $T_1(z_i) = 0$ or $T_2(z_i) = 0$. These values determine four horizontal planes $\zeta_i\colon z = z_i$ that intersect $\mathcal{H}_1$ and $\mathcal{H}_2$ in circles $S_1(z_i)$ and $S_2(z_i)$ which are tangent to each other.

In the following we will show that the polynomial $c(z) := T_1(z)T_2(z)$ is suitable to replace the polynomial of degree four f to distinguish the cases of Theorem 1.

Theorem 2. *If the intersection of H_1 and H_2 is non-empty, the number of real roots of the quartic polynomial $g(t) = \det(t\mathbf{H}_1 + \mathbf{H}_2)$ and of the two circle tangent conditions* (9) *is equal.*

Proof. With respect to suitably chosen coordinate frames in the fixed and moving system, the roots of $g(t)$ can be computed explicitly (see Bottema and Roth [2, Chapter 11.8]). We choose the fixed coordinate frame such that

$$(\xi_1, \eta_1)^T = (-\xi/2, 0)^T \quad \text{and} \quad (\xi_2, \eta_2)^T = (\xi/2, 0)^T \tag{10}$$

and the moving coordinate frame so that

$$(a_1, b_1)^T = (-a/2, 0)^T \quad \text{and} \quad (a_2, b_2)^T = (a/2, 0)^T. \tag{11}$$

This means that $\xi > 0$ is the length of the base link and $a > 0$ is the length of the coupler link. The input and output links are of length r_1 and r_2, respectively.

Now we introduce the abbreviation $[\circ \star \bullet] = r_1 \circ r_2 \star a \bullet \xi$ where the symbols "$\circ$", "$\star$", "$\bullet$" are either "$+$" or "$-$" and compute the four roots of $g(t)$:

$$\begin{aligned} v_{0,1} &= \frac{1}{2r_1^2}\Big((a+\xi)^2 - r_1^2 - r_2^2 \pm \sqrt{[+++][---][+--][-++]}\Big), \\ v_{2,3} &= \frac{1}{2r_1^2}\Big((a-\xi)^2 - r_1^2 - r_2^2 \pm \sqrt{[+-+][-+-][++-][--+]}\Big). \end{aligned} \tag{12}$$

type	real roots	assembly modes
non-Grashof	2	1
crank-rocker/rocker-crank	4	2
double-rocker/double-crank	0	2

Table 1: Linkage type and number of real solutions

On the other hand, the roots of the circle tangent conditions (9) are

$$\zeta_{0,1} = \pm\sqrt{-\frac{[+-+][+++]}{[+++][+--]}} \quad \text{and} \quad \zeta_{2,3} = \pm\sqrt{-\frac{[--+][-+-]}{[-++][---]}}. \tag{13}$$

Because $H_1 \cap H_2$ has real points, there exist physical realizations of the corresponding four-bar mechanism. Hence the sum of any three link lengths is larger than the fourth link length. This is equivalent to

$$[++-] > 0, \quad [+-+] > 0, \quad [-++] > 0, \quad [---] < 0. \tag{14}$$

The inequality $[+++] > 0$ holds because all link lengths are assumed positive. Now it is easy to see that ν_0 and ν_1 are real iff $[+--] < 0$ and complex otherwise. The same is true for ζ_0 and ζ_1. ν_2 and ν_3 are real iff $[-+-][--+] > 0$ and complex otherwise. The same is true for ζ_2 and ζ_3. □

As consequence of Theorem 1 and Theorem 2 we can state

Corollary 1. *It is possible to replace $f(t)$ by $c(z) = T_1(z)T_2(z)$ when applying Theorem 1 to the intersection curve C of $\mathcal{H}_1$ and $\mathcal{H}_2$.*

Remark 2. In order to compute the morphology of the intersection curve of two general quadrics $\mathcal{A}$ and $\mathcal{B}$, we have to compute the number of real roots of a polynomial of degree four. In the special case of two hyperboloids $\mathcal{H}_1$ and $\mathcal{H}_2$ of the shape (5) we only have to compute the number of real roots of the two quadratic polynomials (9). This problem has a simple solution in closed form. Using Equation (12) is not as convenient because the special positions of fixed and moving frame are not readily available although their computation would not be difficult.

Remark 3. A complicated proof Theorem 2 is already given in Schröcker et al. [14]. This proof makes heavy use of a computer algebra system to show that the cross-ratios of the roots ν_i and ζ_i are identical. From this it is deduced that the number of real roots of (12) and (13) is the same.

Remark 4. The proof of Theorem 2 can be used for discussing how the number of real roots in (12) or (13) is related to the type of the synthesized mechanism. Since precisely this discussion has already been carried out in Bottema and Roth [2, Chapter 11.8], we simply display the results in Table 1. Concerning the terminology, we refer the reader to Erdman et al. [5].

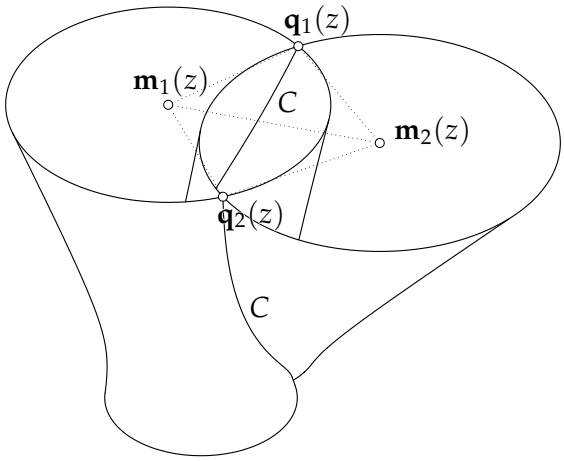

Figure 2: The two branches of the intersection curve C can be distinguished by the orientation of the triangles $\mathbf{m}_1\mathbf{m}_2\mathbf{q}_1$ and $\mathbf{m}_1\mathbf{m}_2\mathbf{q}_2$.

4 Distribution of precision points

In the preceding section we have developed a criterion for deciding whether the intersection curve C of the hyperboloids $\mathcal{H}_1$ and $\mathcal{H}_2$ consists of one or two branches. In this section we give a criterion to decide whether two given points $\mathbf{p}_1$, $\mathbf{p}_2 \in C$ lie on the same or different branches of C. This allows an assembly mode decision directly in kinematic image space. Thereby, the horizontal planes ζ_i that intersect $\mathcal{H}_1$ and $\mathcal{H}_2$ in tangent circles $S_1(z_i)$ and $S_2(z_i)$ play an important role.

It will be convenient to consider the z-values of horizontal planes as elements of the projective line $\overline{\mathbb{R}} = \mathbb{R} \cup \{\infty\}$. A closed interval of z-values is either a closed interval of $\mathbb{R}$ or the union of sets $(-\infty, z_0]$, $[z_1, \infty)$ and $\{\infty\}$ (a projective interval). Via stereographic projection, projective intervals can be visualized as intervals on a circle. The value ∞ is considered to be a zero of (9) if the leading coefficient of the respective quadratic equation vanishes.

We denote the number of real zeros of the circle tangent conditions by ψ. In order to decide whether the points $\mathbf{p}_1$ and $\mathbf{p}_2$ lie in one connected component, we distinguish three cases (see also Figure 1):

Case 1: $\psi = 2$

By Corollary 1, the intersection curve C of $\mathcal{H}_1$ and $\mathcal{H}_2$ has only one connected component (middle image in Figure 1). The corresponding four-bar is of non-Grashof type and has only one assembly mode. An assembly mode decision is not necessary.

Case 2: $\psi = 0$

By Corollary 1, C consists of two affinely infinite branches. Therefore, every real horizontal plane intersects C in the absolute circle points at infinity and two further real points $\mathbf{q}_1(z)$ and $\mathbf{q}_2(z)$, one on every branch of C (Figure 2). Since these points never coincide, they never lie on the connecting line of $\mathbf{m}_1(z)$ and $\mathbf{m}_2(z)$ and the two branches can be distinguished by the orientation of the triangles $\mathbf{m}_1\mathbf{m}_2\mathbf{q}_1$ and $\mathbf{m}_1\mathbf{m}_2\mathbf{q}_2$ (see Figure 2). In order to compute the orientations, we denote the projections of $\mathbf{m}_i(z)$ and $\mathbf{q}_i(z)$ onto the plane $z = 0$ by $\mathbf{m}_i'(z)$ and $\mathbf{q}_i'(z)$. The two branches of C can be distinguished by the sign of the determinant

$$\Delta(z) = \det\big(\mathbf{m}_1'(z) - \mathbf{q}_i'(z), \mathbf{m}_2'(z) - \mathbf{q}_i'(z)\big). \tag{15}$$

In order to decide whether the precision points $\mathbf{p}_1$ and $\mathbf{p}_2$ lie in one assembly mode we substitute them into the determinant (15) with $\mathbf{q}_i(z) = \mathbf{p}_i$ and z as the third coordinate of $\mathbf{p}_i$. If and only if the two determinants have the same sign, the precision points lie on the same branch of C.

Case 3: $\psi = 4$

By Corollary 1, C consists of two affinely finite branches. A real horizontal plane intersects C in the absolute circle points at infinity and two further points, real or complex. By reasons of continuity, the z-values where both points are real define two disjoint intervals of $\overline{\mathbb{R}}$, corresponding to the two branches of C. In order to decide whether $\mathbf{p}_1$ and $\mathbf{p}_2$ lie on the same branch of C, we have to test whether their z-coordinates lie in the same projective interval or not.

5 Comments on the proposed assembly mode test

An overview of existing methods of assembly mode identification of four-bar mechanisms is given in Mirth and Chase [9, Section "Available Solutions to the 'Branch Defect'"]. The main advantages of our approach is that it works directly in kinematic image space. This has important consequences:

- Combined with the algorithm of Brunnthaler et al. [3], the proposed algorithm allows synthesis and assembly mode decision in a homogeneous design environment (kinematic image space).
- Our algorithm avoids computing the mechanism dimensions. Therefore, the assembly mode decision is possible at an early stage of the design process. Because the mechanism dimensions are not used, identification of crank links, computation of input angles for prescribed positions or mechanism inversion can be avoided completely.

Additionally, the proposed algorithm uses only simple arithmetic operations and can be performed without resorting to numerical methods.

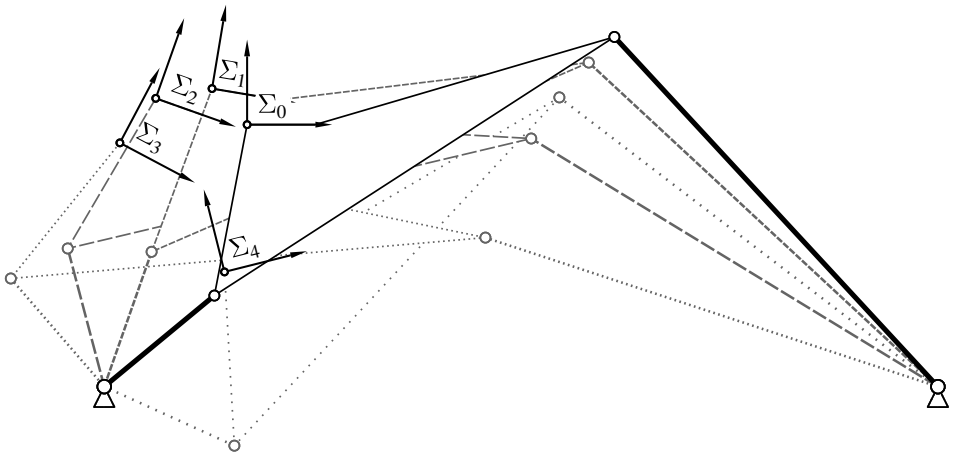

Figure 3: Input positions and four-bar to C_{23} (non-Grashof) for Example 1

6 Examples

In this section we illustrate the presented algorithm for making assembly mode decisions with three examples. They demonstrate how the kinematic mapping based evaluation of assembly modes can be used during the design of four-bar mechanisms.

The general procedure is as follows: Following Brunnthaler et al. [3], we compute up to four real hyperboloids $\mathcal{H}_j$ of the shape (4) through the kinematic images $\mathbf{p}_i$ of the input precision points. Then we apply our algorithm to the five points $\mathbf{p}_i$ and any of the pairs $(\mathcal{H}_j, \mathcal{H}_k)$, sorting out those with an assembly mode defect.

Example 1: One branch

We consider the five input poses

$$\begin{aligned} a_1 &= 0.0000, & b_1 &= 0.0000, & \varphi_1 &= 0.0000, \\ a_2 &= -1.4728, & b_2 &= 1.5135, & \varphi_2 &= -0.1654, \\ a_3 &= -3.8355, & b_3 &= 1.1048, & \varphi_3 &= -0.3410, \\ a_4 &= -5.3417, & b_4 &= -0.7647, & \varphi_4 &= -0.4880, \\ a_5 &= -0.9496, & b_5 &= -6.1825, & \varphi_5 &= 0.2460 \end{aligned} \tag{16}$$

(see Figure 3).[1] Their kinematic images are

$$\begin{aligned} \mathbf{p}_1 &= (0.0000, 0.0000, 0.0000)^T, & \mathbf{p}_2 &= (-0.6957, -0.7991, -0.0829)^T, \\ \mathbf{p}_3 &= (-0.2222, -2.0129, -0.1722)^T, & \mathbf{p}_4 &= (1.0473, -2.5757, -0.2490)^T, \\ \mathbf{p}_5 &= (3.0326, -0.8570, 0.1236)^T. \end{aligned} \tag{17}$$

[1] Note that is no restriction of generality to assume one of the input poses is the identity. This can always be achieved by a suitable coordinate transformation in the fixed frame.

	ζ_0	ζ_1	ζ_2, ζ_3
C_{01}	0.1267	-0.8423	$-0.2919 \pm 0.1099\mathrm{i}$
C_{02}	0.1623	-0.4700	$-0.1284 \pm 0.2929\mathrm{i}$
C_{03}	-0.5345	0.5879	$0.0198 \pm 0.1581\mathrm{i}$
C_{12}	0.5684	-0.5159	$0.0203 \pm 0.0377\mathrm{i}$
C_{13}	-0.4682	0.1607	$-0.1401 \pm 0.0172\mathrm{i}$
C_{23}	-1.1558	0.2914	$-0.2912 \pm 0.1198\mathrm{i}$

Table 2: Roots of the circle tangent conditions in Example 1

Following Brunnthaler et al. [3], we synthesize the four-bar mechanisms guiding the coupler through these positions. It turns out that there exist six real solutions. In kinematic image space, they correspond to the intersection curves $C_{ij} = H_i \cap H_j$ of two of the hyperboloids $H_k \colon \mathbf{x}^T \cdot \mathbf{H}_k \cdot \mathbf{x}$ where

$$\begin{aligned}
\mathbf{H}_1 &= \begin{bmatrix} 0.0000 & -29.3645 & -27.1602 & 552.7938 \\ -29.3645 & 4.0000 & 0.0000 & -88.8388 \\ -27.1602 & 0.0000 & 4.0000 & 14.6364 \\ 552.7938 & -88.8388 & 14.6364 & 1626.6497 \end{bmatrix}, \\
\mathbf{H}_2 &= \begin{bmatrix} 0.0000 & -7.6444 & 9.2472 & 55.8470 \\ -7.6444 & 4.0000 & 0.0000 & 14.7438 \\ 9.2472 & 0.0000 & 4.0000 & 36.3457 \\ 55.8470 & 14.7438 & 36.3457 & 348.6098 \end{bmatrix}, \\
\mathbf{H}_3 &= \begin{bmatrix} 0.0000 & -21.6825 & 38.6344 & 133.0142 \\ -21.6825 & 4.0000 & 0.0000 & 108.9486 \\ 38.6344 & 0.0000 & 4.0000 & 74.9160 \\ 133.0142 & 108.9486 & 74.9160 & 3879.8633 \end{bmatrix}, \\
\mathbf{H}_4 &= \begin{bmatrix} 0.0000 & 768.9417 & 84.0047 & -12054.2749 \\ 768.9417 & 4.0000 & 0.0000 & -18.2336 \\ 84.0047 & 0.0000 & 4.0000 & -407.0783 \\ -12054.2749 & -18.2336 & -407.0783 & -108070.7116 \end{bmatrix}.
\end{aligned} \tag{18}$$

For any pair of hyperboloids the roots of the circle tangent conditions (9) are given in Table 2. We see that there are always two real and two complex roots. Therefore, the five input positions (16) can be reached by six non-Grashof mechanisms that have only one assembly mode. The solution mechanism to C_{01} is depicted in Figure 3.

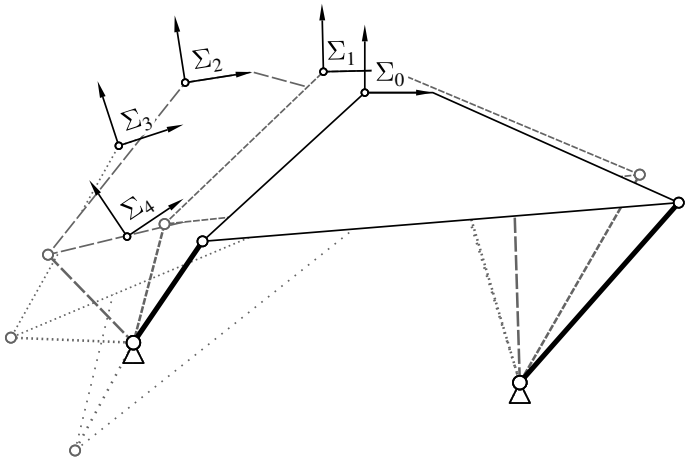

Figure 4: Input positions and synthesized four-bar (crank-rocker) for Example 2

Example 2: Two affinely finite branches

We consider the five input poses

$$\begin{aligned} a_1 &= 0.0000, & b_1 &= 0.0000, & \varphi_1 &= 0.0000, \\ a_2 &= -1.7373, & b_2 &= 0.8786, & \varphi_2 &= 0.0225, \\ a_3 &= -7.5382, & b_3 &= 0.4206, & \varphi_3 &= 0.1557, \\ a_4 &= -10.3289, & b_4 &= -2.2305, & \varphi_4 &= 0.3169, \\ a_5 &= -9.9802, & b_5 &= -6.0441, & \varphi_5 &= 0.5906 \end{aligned} \tag{19}$$

(see Figure 4). Their kinematic images are

$$\begin{aligned} \mathbf{p}_1 &= (0.0000, 0.0000, 0.0000)^T, & \mathbf{p}_2 &= (-0.4491, -0.8637, 0.0113)^T, \\ \mathbf{p}_3 &= (-0.5044, -3.7527, 0.0780)^T, & \mathbf{p}_4 &= (0.2899, -5.3427, 0.1598)^T, \\ \mathbf{p}_5 &= (1.5040, -5.9094, 0.3042)^T. \end{aligned} \tag{20}$$

Following Brunnthaler et al. [3], we synthesize six four-bar mechanisms guiding the coupler through these positions. It turns out that there exists only one real solution (Figure 4). In kinematic image space, it corresponds to the intersection curve $C = H_1 \cap H_2$ of the two hyperboloids $H_i \colon \mathbf{x}^T \cdot \mathbf{H}_i \cdot \mathbf{x}$ where

$$\begin{aligned} \mathbf{H}_1 &= \begin{bmatrix} 0.0000 & -15.1078 & 13.3466 & 260.7857 \\ -15.1078 & 4.0000 & 0.0000 & -39.3775 \\ 13.3466 & 0.0000 & 4.0000 & 33.5844 \\ 260.7857 & -39.3775 & 33.5844 & 568.0302 \end{bmatrix}, \\ \mathbf{H}_2 &= \begin{bmatrix} 0.0000 & -8.5054 & 5.8011 & -21.7319 \\ -8.5054 & 4.0000 & 0.0000 & 33.0529 \\ 5.8011 & 0.0000 & 4.0000 & 33.4765 \\ -21.7319 & 33.0529 & 33.4765 & 526.7938 \end{bmatrix}. \end{aligned} \tag{21}$$

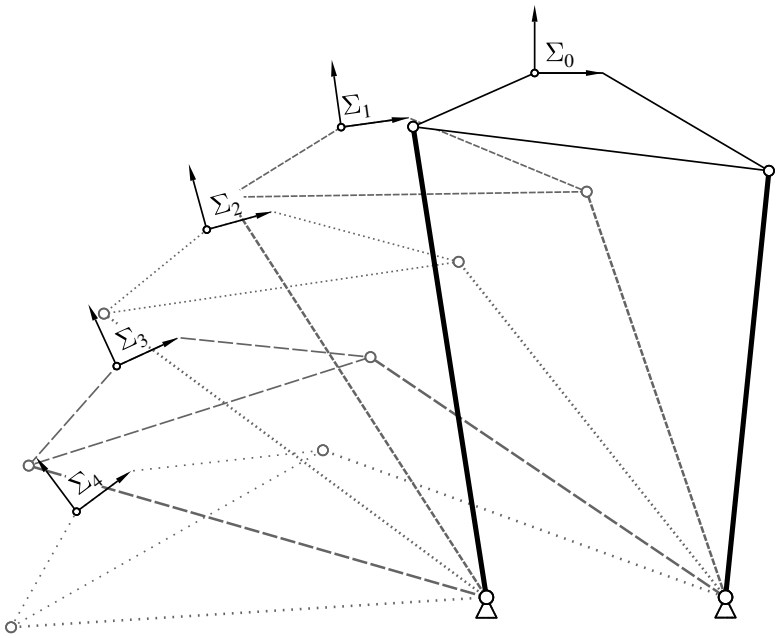

Figure 5: Input positions and synthesized four-bar (double-crank) for Example 3

In order to make an assembly mode decision, we compute the circle tangent conditions

$$T_1(z)\colon z^2 + 0.2218z - 0.1915 = 0, \quad T_2(z)\colon z^2 + 0.1861z + 0.0006 = 0. \tag{22}$$

and their zeros

$$\chi_0 = 0.3405, \quad \chi_1 = -0.5623, \quad \chi_2 = -0.0034, \quad \chi_3 = -0.1826. \tag{23}$$

All zeros are real and the z-coordinates of the precision points (20) lie between χ_2 and χ_0. Therefore, all input poses can be reached within the same assembly mode. The synthesized four-bar is depicted in Figure 4. According to Table 1, the mechanism is expected to be a crank-rocker or rocker-crank which is indeed the case.

Example 3: Two affinely infinite branches

We consider the five input poses

$$\begin{aligned}
a_1 &= 0.0000, & b_1 &= 0.0000, & \varphi_1 &= 0.0000,\\
a_2 &= -8.1232, & b_2 &= -2.2735, & \varphi_2 &= 0.1384,\\
a_3 &= -13.7635, & b_3 &= -6.5753, & \varphi_3 &= 0.2683,\\
a_4 &= -17.5448, & b_4 &= -12.3036, & \varphi_4 &= 0.4307,\\
a_5 &= -19.2319, & b_5 &= -18.4136, & \varphi_5 &= 0.6396
\end{aligned} \tag{24}$$

(see Figure 5). Their kinematic images are

$$\begin{aligned} \mathbf{p}_1 &= (0.0000, 0.0000, 0.0000)^T, & \mathbf{p}_2 &= (0.8552, -4.1404, 0.0693)^T, \\ \mathbf{p}_3 &= (2.3589, -7.3255, 0.1350)^T, & \mathbf{p}_4 &= (4.2329, -10.1181, 0.2187)^T, \\ \mathbf{p}_5 &= (6.0223, -12.6649, 0.3312)^T. \end{aligned} \tag{25}$$

Following Brunnthaler et al. [3], we synthesize six four-bar mechanisms guiding the coupler through these positions. It turns out that there exists only one real solution (Figure 5). In kinematic image space, it corresponds to the intersection curve $C = H_1 \cap H_2$ of the two hyperboloids $H_i \colon \mathbf{x}^T \cdot \mathbf{H}_i \cdot \mathbf{x}$ where

$$\begin{aligned} \mathbf{H}_1 &= \begin{bmatrix} 0.0000 & -35.8007 & 3.6480 & 367.1466 \\ -35.8007 & 4.0000 & 0.0000 & -35.7000 \\ 3.6480 & 0.0000 & 4.0000 & 52.2201 \\ 367.1466 & -35.7000 & 52.2201 & 676.6073 \end{bmatrix}, \\ \mathbf{H}_2 &= \begin{bmatrix} 0.0000 & -39.5146 & -6.1559 & -215.4515 \\ -39.5146 & 4.0000 & 0.0000 & 14.2494 \\ -6.1559 & 0.0000 & 4.0000 & 48.5306 \\ -215.4515 & 14.2494 & 48.5306 & 239.7407 \end{bmatrix}. \end{aligned} \tag{26}$$

In order to make an assembly mode decision, we compute the circle tangent conditions

$$T_1(z) \colon z^2 + 0.0915z + 1.7349 = 0, \quad T_2(z) \colon z^2 - 0.1198z + 0.0377 = 0 \tag{27}$$

and their zeros

$$\chi_{0,1} = -0.0458 \pm 1.3164\mathrm{i}, \quad \chi_{2,3} = 0.0599 \pm 0.1846\mathrm{i}. \tag{28}$$

All zeros are complex and we have to compare the signs of the determinants $\Delta(z_i)$ of (15) where z_i are the z-coordinates of the input precision points (25). We compute

$$\begin{aligned} \Delta(z_0) &= 22.7834, & \Delta(z_1) &= 21.7682, & \Delta(z_2) &= 23.5983, \\ \Delta(z_3) &= 29.1426, & \Delta(z_4) &= 40.0435. \end{aligned} \tag{29}$$

All determinants are positive and the assembled mechanism can reach all prescribed positions within one assembly mode. According to Table 1, the mechanism is expected to be a double-rocker or double-crank which is indeed the case (it is a double-crank).

7 Conclusion and future research

In this paper, we exploit the circular shape of the two hyperboloids that intersect to define the image curve of the coupler movement of a four-bar linkage in a kinematic image space. Theorem 2 shows that the simple condition for tangency of circles (9) can be used to classify this image curve for a design solution. This classification identifies whether the image curve has one or two branches, and yields formulas that allow us to

determine if two task positions lie on the same assembly mode. Examples illustrate the use of these formulas.

In a future publication we will shown that the presented method can be adapted to make assembly mode decisions for spherical four-bars.

References

[1] Blaschke W., 1911, "Euklidische Kinematik und nichteuklidische Geometrie," *Zeitschr. Math. Phys.*, 60, pp. 61–91 and 203–204.

[2] Bottema O., and Roth B., 1990, *Theoretical Kinematics*, Dover Publications.

[3] Brunnthaler K., Pfurner M., and Husty M., 2005, "Synthesis of Planar Four-Bar Mechanisms". In Proceedings of MUSME 2005, the International Symposium on Multibody Systems and Mechatronics, Uberlândia, Brazil, 6–9 March 2005.

[4] DaLio M., Cossalter V., and Lot R., 2000, "On the use of natural coordinates in optimal synthesis of mechanisms," *Mech. Mach. Theory*, 35, pp. 1367–1389.

[5] Erdman A. G., Sandor G. N., and Kota S., 2001, *Mechanism Design: Analysis and Synthesis*, Volume 1, 4th Edition, Prentice Hall.

[6] Grünwald J., 1911, "Ein Abbildungsprinzip, welches die ebene Geometrie und Kinematik mit der räumlichen Geometrie verknüpft," *Sitzungsber. Akad. Wiss. Wien*, 120, pp. 667–741.

[7] Gupta K. C., 1980, "Synthesis of position, path and function generating 4-bar mechanisms with completely rotatable driving links," *Mech. Mach. Theory*, 15, pp. 93–101.

[8] Hayes M. J. D., and Zsombor-Murray P. J., 2002, "Solving the Burmester problem using kinematic mapping". Proceedings of ASME DECT'02, Montreal (Montreal, Canada).

[9] Mirth J. A., and Chase T. R., 1993, "Circuits and branches of single-degree-of freedom planar linkages," *ASME Journal of Mechanical Design*, 115, pp. 223–230.

[10] Perez A., and McCarthy J. M., 2005, "Clifford algebra exponentials and planar linkage synthesis equations," *ASME Journal of Mechanical Design*, 127(5) pp. 931–940.

[11] Prentis J. M., 1991, "The pole triangle, Burmester theory and order and branching problems II: The branching problem," *Mech. Mach. Theory*, 26(1), pp. 31–39.

[12] Ravani B., and Roth B., 1983, "Motion synthesis using kinematic mapping," *ASME J. of Mechanisms, Transmissions, and Automation in Design*, 105(3), pp. 460–467.

[13] Schaefer R. S., and Kramer S. N., 1979, "Selective precision synthesis of planar mechanisms satisfying position and velocity constraints," *Mech. Mach. Theory*, 14(3), pp. 161–170.

[14] Schröcker H.-P., and Husty M. and McCarthy, J. M., 2005, *Kinematic Mapping Based Evaluation of Assembly Modes for Planar Four-Bar Synthesis*, Proceedings of ASME 2005 29th Mechanisms and Robotics Conference, Long Beach.

[15] Sommerville D. M. Y., 1934, *Analytical Geometry of Three Dimensions*, Cambridge University Press, London.

[16] Tu C., Wang W., and Wang J., 2002, "Classifying the Morphology of the Nonsingular Intersection Curve of Two Quadric Surfaces". In Proceedings of Geometric Modeling and Processing, Theory and Applications, H. Suzuki and R. Martin, eds., pp. 23–32.

[17] Tu C., Wang W., Mourrain B. and Wang J., 2005, "Signature sequence of intersection curve of two quadrics for exact morphological classification". Technical report, University of Hong Kong, HKU CS Tech Report TR-2005-09.

[18] Waldron K. J., 1976, "Elimination of the branch problem in graphical Burmester mechanism synthesis for four finitely separated positions." *ASME Journal of Mechanical Design* 98(1), pp. 176–182.

[19] Waldron K. J., and Strong R. T., 1978, "Improved solutions of the branch and order problems of Burmester linkage systems." *Mechanism and Machine Theory* 13, pp. 199–207.

[20] Waldron K. J, and Stevenson E. N. Jr., 1979, "Elimination of branch, Grashof and order defects in path-angle generation and function generation synthesis." *J. Mech. Design* 101, pp. 428–437.